Flux Surface Mapping in LHD

Tomohiro MORISAKI, Mamoru SHOJI, Suguru MASUZAKI, Satoru SAKAKIBARA,
Hiroshi YAMADA, Akio KOMORI, Osamu MOTOJIMA
and the LHD experimental group

National Institute for Fusion Science, Toki, Gifu 509-5292 Japan

Magnetic flux surface measurements have been carried out in the Large Helical Device (LHD) in the standard magnetic field configuration with toroidal magnetic field strength up to 2.75 T. Electron beam launched with a small electron gun moving across the flux surfaces was detected with a fluorescent screen or a probe array. Nested surfaces could clearly be visualized with both methods. Even the open ergodic region was also detected. In the experiment an unfavorable m/n = 1/1 magnetic island was found to exist near the last closed flux surface (LCFS), where m and n are poloidal and toroidal mode numbers, respectively. It was found that the source of the error field, in the low magnetic field strength of 0.0875 T, is terrestrial magnetism. On the other hand, in the standard magnetic field strength of 2.75 T, the main source of the error field is though to be ferromagnetic materials near the LHD. It was also found that such magnetic islands can be eliminated or reduced applying the correction field with some perturbation coils.

Keywords: flux surface mapping, magnetic island, ergodic layer

1. Introduction

Unlike tokamaks, helical devices, e.g. heliotron, stellarator, torsatron, do not need a plasma current to form the magnetic flux surfaces for the plasma confinement. These devices can thoroughly achieve the confinement configuration only by their external coils. This means that the magnetic flux surfaces exist in vacuum without any plasma current, thus one can easily identify or measure them, visualizing each surface with a proper instrument installed in the vacuum vessel. Several experiments to map the flux surfaces have been performed in major helical devices with various techniques [1-8]. The Large Helical Device (LHD) is a superconducting heliotron [9], which is by far a favorable device for the flux surface mapping experiment because the standard high magnetic field (~ 3 T) can be maintained in steady state during the mapping experiment.

In this paper, results of the flux surface mapping experiment on LHD are presented. The measurements have been performed in two different methods since the very early phase of the LHD experiment in 1998. In section 2, experimental apparatus and geometry are shown. After describing the experimental results in section 3, discussion is given in section 4. Finally summary is given in section 5.

2. Experimental Apparatus

The principle of the experiment is simple and clear. The electron beam launched on a flux surface from a small electron gun (e-gun) traces a magnetic field line. Projecting the positions on the poloidal plane, where the electron beam passes through, the flux surface is visualized. To identify the piercing points on the poloidal plane, two methods were employed in the experiment.

2.1 Electron Gun

In order to launch the electron beam, a small electron gun (e-gun) was utilized. For two different methods, i.e. fluorescent screen and probe array, two

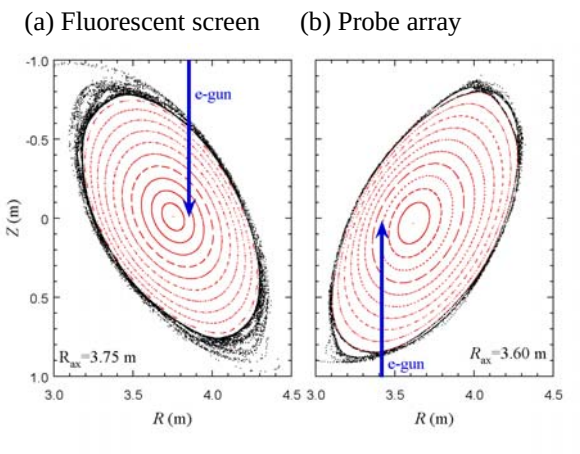

Fig. 1 Position of the e-gun scanning in the poloidal plane in the case of (a) fluorescent screen and (b) probe array methods. The e-gun can be inserted up to ρ = ~ 0.1 with the fluorescent screen method.

author's e-mail: morisaki@nifs.ac.jp

distinct ports to install the e-gun were utilized, as shown in Fig. 1. Moving radailly in the poloidal plane, the e-gun can reach as far as ρ = ~ 0.1 for the fluorescent screen method and ~ 0.3 for the probe array method, where ρ is a normalized minor radius. One can trace different flux surfaces by changing the radial position of the e-gun. For the precise alignment of the electron beam with a magnetic field line, the direction of the e-gun can also be changed, rotating on the supporting rod, since the magnetic shear is very high in the heliotron configuration.

The e-gun itself consists of a lanthanum hexaboride (LaB_6) cathode and a tantalum plate with a 3 mm diameter hole to extract electrons. The cathode is heated up to 1400 K and negatively biased at ~ 150 V to the ground (vacuum vessel). Although no mechanism to collimate or focus electron beams is equipped with, practical beam width (FWHM) is about 10 mm at B_t = 2.75 T, where B_t is the toroidal magnetic field strength.

2.2 Fluorescent Screen and Probe Array

In order to identify the positions where the electron beam passes through a poloidal plane, a fluorescent screen or a scanning probe array was employed.

The screen is made of 70 - 80 % transparent mesh coated with fluorescent powder P15 (ZnO: Zn). The electron beam glows on the screen mesh, circling along the torus for many times. The images on the screen in the poloidal plane are captured with a CCD detector viewing from the tangential port. Changing the radial position of the e-gun, the captured images of each flux surface are superimposed on one picture. Though this method is very simple and straight forward, it is restricted to the configuration between screen and CCD to be seen each other through the viewing window.

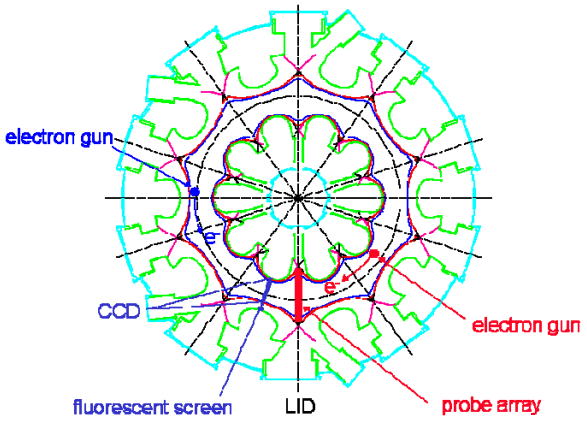

Fig. 2 Geometrical setup of flux surface mapping. Electron beam is launched in the clockwise direction for the probe array and the counterclockwise direction for the fluorescent screen.

If one cannot obtain such a configuration mentioned above, there is another way to detect the electron beam. We introduced an 89 channel vertical probe array to measure the electron current on a flux surface. By scanning it in the horizontal direction, two-dimensional information which consists of 89 horizontal chords on the poloidal plane can be obtained. With this method, no viewing port is necessary, thus we do not have to mind about the geometrical problem. The diameter of each probe chip is 7.8 mm and the distance between adjacent chips is 9 mm. Since the orbit drift of the electron beam with 150 eV is negligibly small compared to the beam width, the spatial resolution of the system is consequently about 10 mm.

2.3 Geometry

The geometrical setup of e-gun, fluorescent screen and probe array is shown in Fig. 2. The fluorescent screen of 2 m high and 1 m wide was installed in the toroidal position where the flux surfaces are vertically elongated. The CCD detector views the screen from the tangential port though the window, as shown in Fig. 2. Although the screen fully covers the poloidal plane of the flux surfaces, the CCD could not perfectly see the whole area of the flux surfaces because of the structure in the vacuum vessel blocking the CCD's view.

On the other hand, the probe array was located at the position where the flux surfaces are horizontally elongated and the Local Island Divertor (LID) [10] head is inserted from outboard side of the torus. Actually the probe head is mounted on the LID head, and travels horizontally with it more than 2 m with the translation mechanism of LID. Thus the 0.8 m high and 2 m wide scanning area covers more than 90 % of the flux surfaces.

3. Experimental Results

Flux surface mapping experiments have been performed three times since the beginning of the LHD experiment in 1998. The magnetic configurations of R_{ax} = 3.60 m, 3.75 m and 3.85 m were chosen for the measurement, where R_{ax} is the magnetic axis position. The B_t was set at B_t = 0.0875 T, 0.25 T and 2.75 T. Note that B_t = 2.75 T is used for the ordinary plasma experiment.

The vacuum vessel was evacuated less than 3×10^{-4} Pa in order to avoid the plasma production along the electron beam. Under this experimental condition, the mean free path of the electron is about 2500 m (100 toroidal turns).

(a) Calculation (b) Experiment

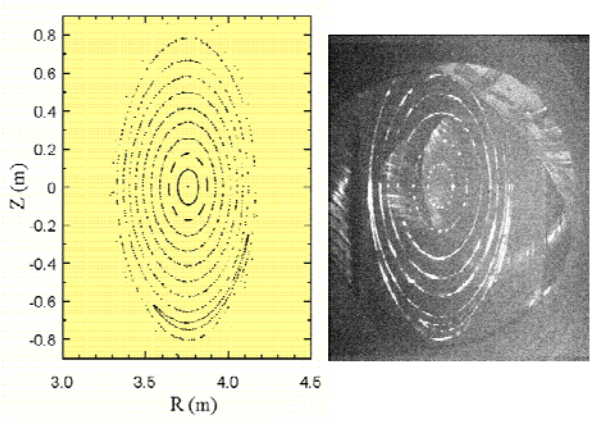

Fig. 3 Flux surfaces (a) calculated with field line tracing code and (b) mapped on the fluorescent screen.

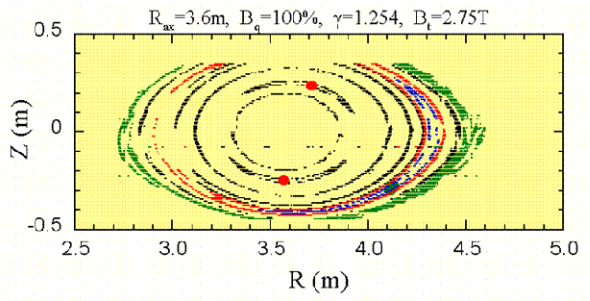

Fig. 4 Flux surfaces measured with 89 ch probe array. Red and blue closed circles are the O-points of m/n = 2/1 and 1/1 magnetic islands, respectively. Separatrix of the 1/1 island is depicted with red line and the ergodic region is colored in green.

3.1 Fluorescent Screen Method

Experimental result of flux surface mapping on the fluorescent screen method is presented in Fig. 3 (b), together with the calculation result with the field line tracing code, as shown in Fig. 3 (a). This experiment was carried out in the standard but low magnetic field configuration, i.e. R_{ax} (average) = 3.75 m and B_t = 0.0875 T. For this result presented in Fig. 3 (b), the position of the e-gun was changed six times and then six pictures were superimposed. It can clearly be seen that the experimental and numerical results agree well. The measured magnetic axis position which was derived by finding the center of each flux surface was found to be at R = 3.77 m where the calculated local magnetic axis position is R = 3.76 m. It can be said that the difference between them is within the error bar of experimental conditions.

It can be seen, unfortunately, that a relatively large magnetic island of which poloidal/toroidal mode numbers are m/n = 1/1. Such a magnetic island is often attributed to the error field caused, for example, by the ferromagnetic materials near the machine or misalignment of the coils. However, in this experiment, the B_t was so low as 0.085 T that it is necessary to take the geomagnetic effect into consideration. In the calculation shown in Fig. 3 (a), the local geomagnetic effect (using published data at Inuyama city near Toki) is taken into account. It is found that the m/n = 1/1 island clearly appears by introducing the terrestrial magnetism in the calculation, and the calculated width and the phase of the magnetic island agree well to the experimental result, as shown in Fig. 3. The cause of the magnetic island will be discussed later again.

3.2 Probe Array Method

Recently the flux surface mapping with an e-gun and a fluorescent screen was performed. As shown in Fig. 4, clear and precise results at the horizontally elongated cross section were obtained with this method. In this experiment, the standard magnetic configuration and magnetic field strength for the usual experiment were employed, i.e. R_{ax} = 3.60 m and B_t = 2.75 T. Outside of the nested closed surfaces depicted in black, it can be seen that complicated ergodic region colored in green spreads out. Such a fine structure has not been observed with the fluorescent screen method.

In spite of high magnetic field of B_t = 2.75 T, the m/n = 1/1 and 2/1 magnetic islands were still observed, as shown in Fig. 4. It is though that these 1/1 and 2/1 islands are toroidally coupled each other. Moving the e-gun precisely, nested closed surfaces within the islands were also detected. Finding one smaller flux surface after another in the island, we could finally reach the smallest magnetic surface at the center of the island, i.e. at the magnetic axis of the island. This is what is called an O-point of the island. In Fig. 4, the O-points of 1/1 and 2/1 island are emphasized by drawing the final smallest flux surface with larger symbols. Concerning the phase of the island (poloidal angle of O-points), it is consistent with that observed in the previous experiment with fluorescent screen, which is described in section 3.1. Thus the island phase calculated with the geomagnetic effect almost agrees to that obtained in the experiment presented in this section. However the relatively large island width shown in Fig. 4 cannot be explained simply by the geomagnetic effect, since B_t is far stronger than terrestrial magnetism. Detailed discussion is presented in the next section.

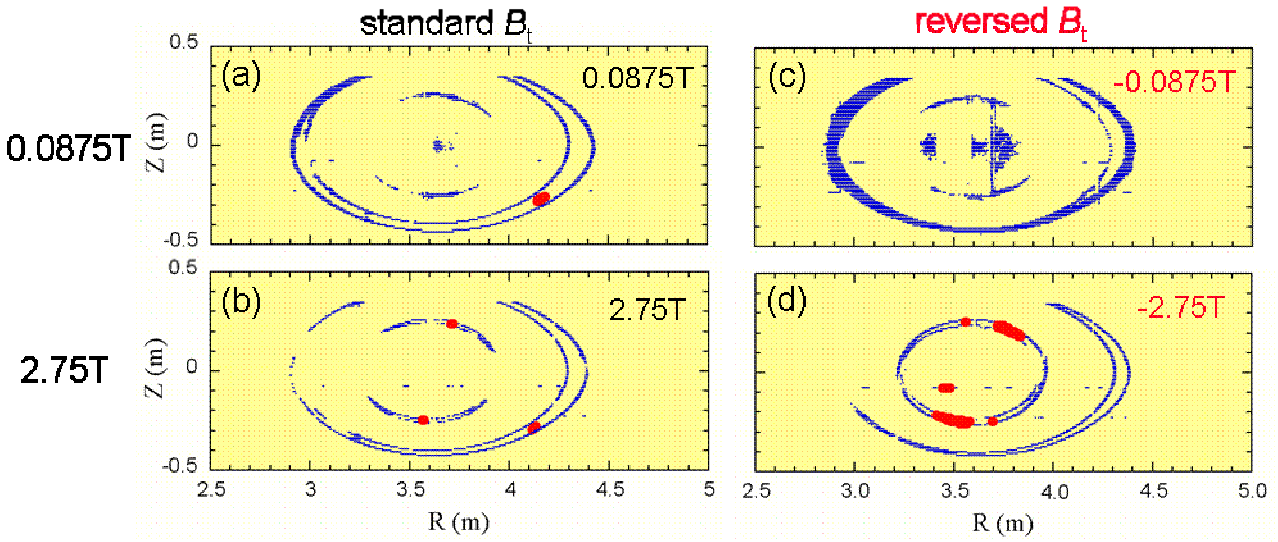

Fig. 5 Variation in magnetic island property under four experimental conditions, i.e. high (2.75 T) and low (0.0875 T) magnetic field strengths, and those reversals. The O-points of each island are emphasized with large red symbols.

4. Discussion

Further investigation for the magnetic islands observed in the flux surface mapping was carried out to find the source of the error field. In order to see the B_t dependence on the island properties, its phase and width were compared between B_t = 0.0875 T and 2.75 T. The direction of B_t was also reversed in each magnetic field strength. Summary of the experiments is presented in Fig. 5. The m/n = 1/1 and 2/1 islands measured with a probe array under four experimental conditions are shown.

Comparing Fig. 5 (a) and (c), it is found that the 1/1 and related 2/1 islands at low B_t are due to weak and steady perturbation, e.g. terrestrial magnetism. This is because, in reversed B_t (Fig.5 (c)), the island phase is also reversed, which suggests the direction of the error field never changes, according to the environmental field.

With increase in B_t, the island width surely decreases, however the decreasing rate is very small, as is seen between Fig. 5 (a) and (b), or between (c) and (d). If the source of the error field were purely from terrestrial magnetism, the island width decreased drastically, because B_t increased more than 30 times between two. This experimental result suggests the existence of another source of the error field, which increases with B_t. Comparing Fig. 5 (b) and (d), another important information can also be seen, namely the island phase never changes, even if B_t is reversed. This means that the direction of the error field changes with B_t direction. Thus we can conclude that there must be another source of the error field in addition to the terrestrial magnetism.

One of the candidates of the error field which has the characteristics mentioned above is the unsaturated ferromagnetic materials near the machine, e.g. magnetic shield for the neutral beam injector and/or diagnostics, deteriorated stainless steel by welding, etc. Fortunately it was also confirmed that these magnetic islands can be eliminated or reduced by using small correction coils.

5. Summary

Flux surface mapping with electron beam and fluorescent screen or probe array was successfully carried out in LHD. It was confirmed that the nested closed surfaces are formed in the standard LHD configuration. The m/n = 1/1 and 2/1 islands were found to exist, but can be eliminated or reduced with small correction coils.

Acknowledgement

This study was partially funded by the Grant Aid for Scientific Research from MEXT of Japanese government.

References

[1] R. M. Sinclair et al., Rev. Sci. Instrum. **41**, 1552 (1970).
[2] G. J. Hartwell *et al.*, Rev. Sci. Instrum. **59**, 460 (1988).
[3] H. Yamada *et al.*, Rev. Sci. Instrum. **61**, 686 (1990).
[4] G. G. Lesnyakov *et al.*, Nucl. Fusion **32**, 2157 (1992).
[5] R. Jaenicke *et al.*, Nucl. Fusion **33**, 687 (1993).
[6] M. G. Shats *et al.*, Nucl. Fusion **34**, 1653 (1994).
[7] H. Lin *et al.*, Rev. Sci. Instrum. **66**, 464 (1995).
[8] M. Otte *et al.*, *Proc. 29th EPS* (ECA, vol.26B, 2002) p-5.036.
[9] O. Motojima *et al.*, Phys. Plasmas **6**, 1843 (1999).
[10] T. Morisaki *et al.*, Phys. Plasmas **14**, 056113 (2007).